

ARTICLE

Measurements of Neutron-production Double-differential Cross-sections at 100 MeV Neutron-Incidence on Fe

Tsuyoshi KAJIMOTO¹, Daisuke MORIGUCHI¹, Yasuhiro NAKAMURA¹, Hiroyuki ARAKAWA¹, Shusaku NODA¹, Nobuhiro SHIGYO¹, Kenji ISHIBASHI¹, Satoshi KUNIEDA², Takehito WATANABE³ and Robert C. HAIGHT³

¹ Department of Applied Quantum Physics and Nuclear Engineering, Kyushu University
744 Motoooka, Nishi-ku, Fukuoka 819-0395 Japan

² Japan Atomic Energy Agency, Tokai, Naka, Ibaraki 319-1195, Japan

³ Los Alamos National Laboratory, Los Alamos, NM 87545, USA

The neutron-induced neutron-production double-differential cross-sections at 100 MeV by bombarding a Fe sample with continuous energy neutron were measured. A fission ionization chamber was set to take the incident-neutron flux. Six NE213 liquid scintillators, 12.7 cm thick and 12.7 cm in diameter, were placed at 15, 30, 60, 90, 120 and 150 to detect neutrons emitted from a sample. Incident energies of neutrons were obtained by the time of flight (TOF) method. The distance from the spallation target to an NE213 scintillator was applied as the flight length of incident neutrons. The energy spectra of emitted neutrons were derived from unfolding their deposition-energy spectra with the response functions of the detectors. The response functions were also measured with the spallation neutrons above neutron energy of 20 MeV. In the unfolding process, neutron-induced neutron-production double-differential cross-sections were approximated by the moving source model. The experimental results were compared with calculations of the PHITS code using the JENDL-HE file.

KEYWORDS: *neutron incident neutron production cross section, spallation, NE213, moving source model*

I. Introduction

Neutron-production double-differential cross-sections for intermediate and high energy region are important for radiotherapy and shielding design of accelerators. Proton-induced neutron-production double-differential cross sections have been measured up to 3 GeV¹⁻³. However, data of neutron-induced neutron-production double-differential cross sections above 100 MeV are insufficient because of neutron measurement difficulties and a few quasi-monochromatic neutron sources. Utilization of a continuous energy neutron source by spallation reaction enables to measure cross sections for various incident energies at a time.

The purpose of this study is to measure the neutron-production double-differential cross sections at 100 MeV neutron-incidence on Fe by using a continuous energy neutron source.

II. Experiments

Experiments were performed at the Weapons Neutron Research (WNR) facility in Los Alamos Neutron Science Center (LANSCE) which has an 800 MeV proton linear accelerator. Neutrons generated at a tungsten spallation target (Target-4) were used as incident particles. The neutron energies cover a wide energy range up to 750 MeV. The distance between the Target-4 and the experimental room is about 90 m. A fission ionization chamber was set to take the incident-neutron flux. NE213 liquid scintillators, 12.7 cm thick and 12.7 cm in diameter, were used to detect neutrons emitted from a sample. Incident energy of neutrons were obtained by the time of flight

(TOF) method. The distance from the Target-4 to an NE213 scintillator was taken as the flight length of incident neutrons because the distance between the Target-4 and the sample was much longer than that between the sample and the detector. The energy spectra of neutrons emitted from the sample was derived by employing an unfolding method.

The experiments consisted of two parts. The first one was the measurement of deposition-energy spectra of neutrons emitted from the sample. A schematic view of the experimental arrangement is illustrated in **Fig. 1**. Six NE213 scintillators were placed at 15, 30, 60, 90, 120 and 150, and employed to detect neutrons emitted from an Fe sample of 10 mm thickness and 50 mm in diameter. The distance between the sample and each detector was about 0.7 m. A 10 mm thick NE102A plastic scintillator as a veto detector was set in front of each NE213 scintillator. The beam size was adjusted to 36 mm in diameter. A fission ionization chamber⁴ was set to know the incident-neutron flux. The TOF spectrum of each NE213 detector and each spectrum of charge amounts of the area of a pulse delivered by the photomultiplier connected with the NE213 scintillator were measured. The other part of the experiments was the measurement of response functions of the NE213 detectors. Because the responses of the NE213 detectors to neutrons have continuous energy spectra, the energy spectra of emitted neutrons were derived from unfolding their deposition-energy spectra with response functions of the NE213 detectors. These response functions were measured by using the spallation neutrons which were collimated to 3.5 mm in diameter. The alignment of the experiment is in **Fig. 2**. The response function of each NE213 detector was measured by irradiating neutrons from the Target-4. In the same way as the foregoing measurement, the TOF spectrum and the charge spectrum were measured.

Corresponding author, E-mail: kajimoto@kune2a.nucl.kyushu-u.ac.jp
c Atomic Energy Society of Japan

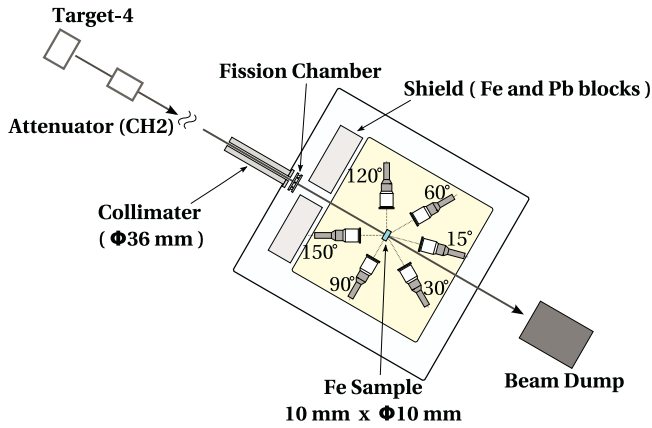


Fig. 1 Arrangement of the measurement for deposition-energy spectra of neutrons emitted from a sample.

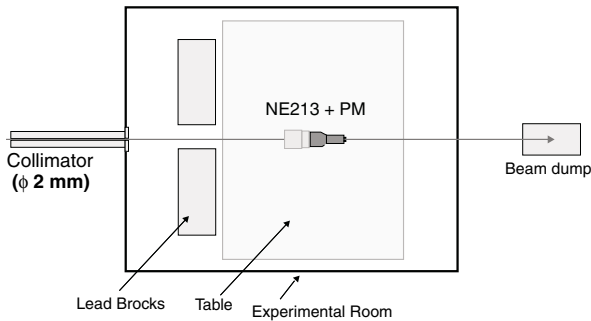


Fig. 2 Arrangement of the measurement for response functions.

III. Analysis

1. Incident neutron numbers

The number of incident neutrons was measured by a ^{238}U fission ionization chamber. Alpha decay events of ^{238}U were eliminated since alpha decay events gave lower charge than that of fission events induced by neutrons. Incident neutron energy were derived from the TOF method. The number of incident neutrons was got by the equation

$$\phi_{\mu p}(E_n)\Delta E_n = \frac{n_f(E_n)\Delta E_n}{\sigma(E_n)\epsilon_{eff}\rho_f n_{\mu p}S_{beam}}, \quad (1)$$

where $\phi_{\mu p}(E_n)$, $n_f(E_n)$, and $\sigma(E_n)$ are the number of incident neutrons, the number of fission events detected by the fission chamber, and the fission cross sections of ^{238}U for corresponding neutron energy E_n ⁵⁾, respectively. ϵ_{eff} is the detection efficiency of the fission chamber, and ρ_f is the density of the number of atoms of fissile material on the foil in chamber. $n_{\mu p}$ is the number of the proton beam with micro pulse. S_{beam} shows the area of the beam.

2. Deposition-energy spectra

In the measurement data of deposition-energy spectra of neutrons emitted from the sample, charged particle events were eliminated since charged particles gave larger energies in an NE102A scintillator than neutrons and gamma-rays.

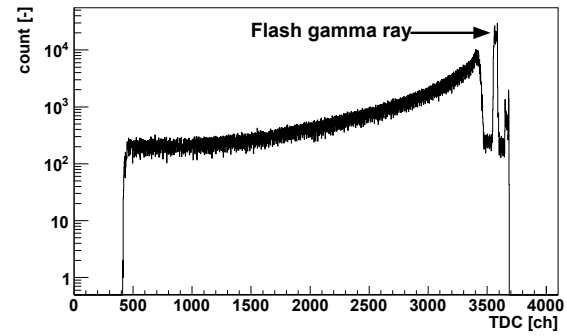


Fig. 3 The TOF spectrum at 15 deposition-energy spectra measurement.

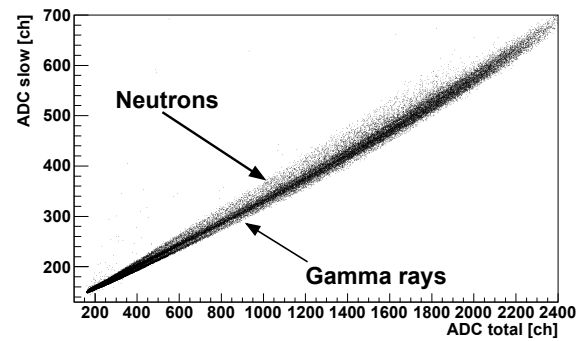


Fig. 4 Two dimensional plots of two ADC outputs at 15 deposition-energy spectra measurement.

Incident neutron energies were converted from neutron flight times between the Target-4 and the NE213 detectors. The flight time between the NE213 detectors and the sample was negligible since the distance between the Target-4 and the sample was much longer than those between the sample and the NE213 detectors. Fig. 3 shows one of the TOF spectra. The timing of flash gamma-rays from the Target-4 was used as the time base of the TOF analysis.

The neutron-gamma discrimination was performed by the two gate integration method. A charge delivered by the photomultiplier was measured by ADCs during two different gate times, which gave two charge amounts data. A two-dimensional plot of charge amounts of total and slow gates was shown in Fig. 4. In the figure, neutron and gamma ray events were not clearly identified. Projections to the delayed gate charges of the two dimensional plot were fitted with two Landau distributions for neutron and gamma ray events. The reason using two Landau distributions was that two Landau distribution gave good agreement with the projection. The neutron-gamma discrimination was performed by the area ratio of two Landau distributions. Fig. 5 shows an example of a projection and results of fitting.

Charge spectra were calibrated to get corresponding electron-equivalent light-output for all neutron detectors. For the calibration of low-energy (a few MeV) parts, the Compton edges of ^{60}Co and Pu-Be sealed gamma-ray sources were

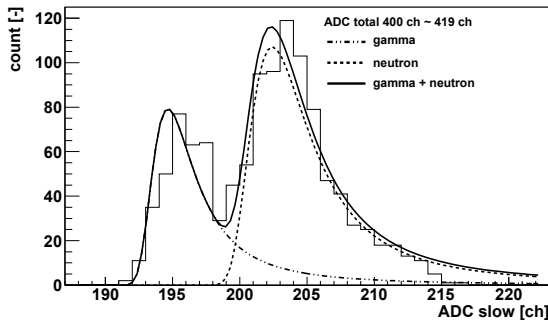


Fig. 5 Projections to the delayed gate charges of the two-dimensional plot and fitting at 15° deposition-energy spectra measurement.

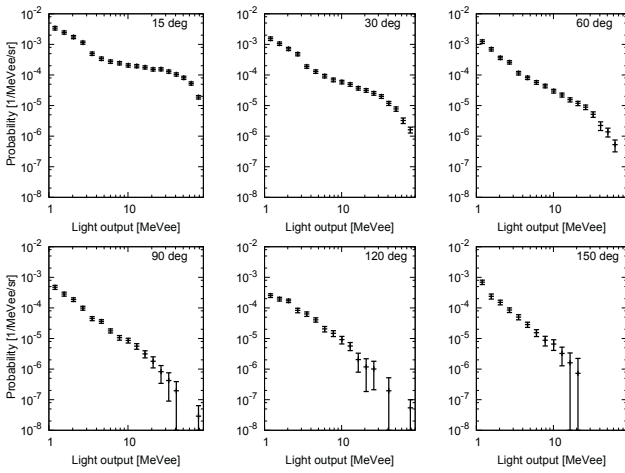


Fig. 6 Deposition-energy spectra at 90 – 110 MeV neutron incident energy.

converted into light-unit with the semi-empirical formula by Dietze et al.⁶⁾. For the calibration of higher-energy parts, conversion from ADC channel into neutron energy was identified by charge spectrum at each incident energy in the response function measurement data since protons generated by interaction with neutrons in the NE213 scintillator gave higher deposition energy than other charged particles. Neutron energies were converted into electron-equivalent light-unit by the empirical equation by Nakao et al.⁷⁾

$$T_e = 0.81T_p - 2.80 \{1.0 - \exp(-0.20T_p)\}, \quad (2)$$

where T_p , T_e are proton and electron energy (MeV) in an NE213 scintillator, respectively.

Deposition-energy spectra at 90 – 110 MeV normalized by the number of incident neutron and subtracted background neutrons obtained without a sample are shown in **Fig. 6**.

3. Response functions of NE213 detectors

In the same way as deposition-energy spectra analysis, we performed derivation of incident neutron energy, neutron-gamma discrimination, and calibration of conversion from ADC channel to electron-equivalent light-outputs.

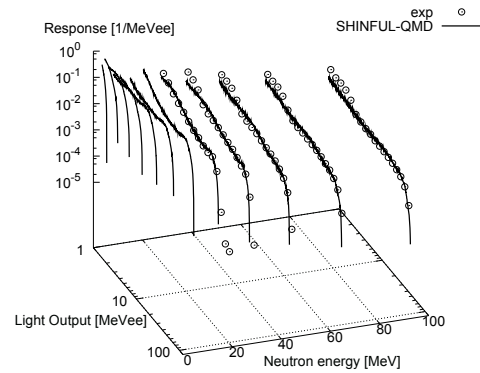


Fig. 7 Response function of the NE213 detector at 120°.

Response functions of NE213 detectors normalized by the number of incident neutrons were shown in **Fig. 7**. In this experiment, the SCINFUL-QMD⁸⁾ calculations adjusted to reproduce the experimental data with light attenuation were used to get the response matrix elements below 20 MeV incident energy for all NE213 detectors since there were no experimental data below 20 MeV incident energies.

4. Unfolding

The energy spectra of emitted neutrons were derived by unfolding their deposition-energy spectra with the response functions of the NE213 detectors. In this experiment, elastic scattering component was considered separately from the other reaction components. The determinant of this experiment was

$$\begin{pmatrix} \vdots \\ y_\xi \\ \vdots \end{pmatrix} = \begin{pmatrix} \ddots & \vdots & \vdots \\ \vdots & a_{\xi,E} & \vdots \\ \vdots & \vdots & \ddots \end{pmatrix} \cdot \begin{pmatrix} \vdots \\ x_E \\ \vdots \end{pmatrix} \cdot k + \begin{pmatrix} \vdots \\ a_{\xi,E_{in}} \\ \vdots \end{pmatrix} \cdot x_{el} \cdot k, \quad (3)$$

where y_ξ , a_ξ , E , and x_E were deposition-energy spectra, response function, and outgoing energy spectra (unfolded results), respectively. x_{el} was the elastic scattering factor. k was the matching factor for absolute value of response functions with deposition-energy spectra. $x_E (=x(E, \theta))$ was assumed to conform the moving source model⁹⁾. **Equation 4** represents the moving source model.

$$\frac{d^2\sigma}{dE d\Omega} = \sum_{i=1}^3 pA_i \exp \left\{ - \left(\frac{E + m - p\beta_i \cos \theta}{\sqrt{1 - \beta_i^2}} - m \right) / T_i \right\} + A_G \exp \left\{ - \frac{(E - E_G)^2}{\sigma_G^2} \right\}, \quad (4)$$

where E and p is the kinetic energy (MeV) and the momentum (MeV/c) of an emitted neutron in the laboratory frame and m the neutron mass (MeV), respectively. The quantities of A , β , and T are called amplitude, velocity and nuclear temperature parameters, respectively. Three components

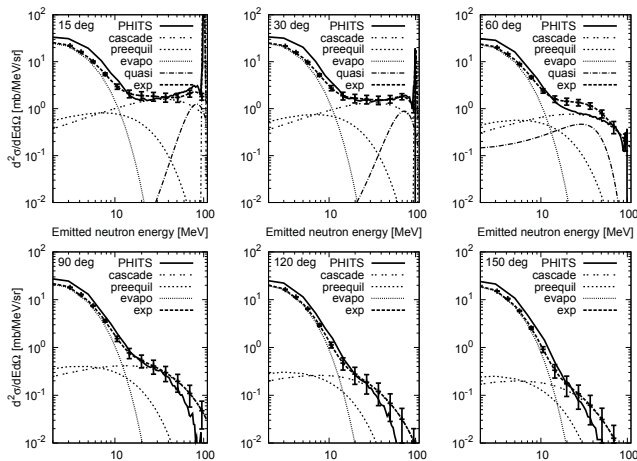


Fig. 8 Double-differential cross sections for 90 – 110 MeV neutron incident energy on Fe with calculated data.

of $i=1$ to 3 correspond to individual processes of the cascade, the preequilibrium and the evaporation. A_G , E_G and σ_G in the last term were adjustable parameters for the quasi-elastic and quasi-inelastic-like scattering components. The quasi-elastic and quasi-inelastic-like scatterings were taken account to data of 15 30 60 . In the process of unfolding, neutron-induced neutron-production double-differential cross sections were parameterized with moving source model by SALS code¹⁰⁾ as a least mean square approximation program.

IV. Results

The provisional parameterized double-differential cross sections by the moving source model with the components for 90 – 110 MeV neutron incident energies were shown in **Fig. 8**. These results were compared with the PHITS¹¹⁾ calculations using the JENDL-HE file¹²⁾. The calculated data roughly reproduced all the experimental data. Under 10 MeV neutron emission energy, the calculated data overestimated all the experimental data. This is attributed not to consider the attenuation effect in a sample for neutrons emitted from a sample. For the elastic components of 15 and 30 , the experimental results were approximately in good agreement with calculated data.

V. Conclusion

The neutron-induced neutron-production double-differential cross sections at 100 MeV on Fe were measured by using a continuous energy neutron source. The double-differential cross sections were parameterized by the moving source model. The experimental data were compared with

calculated data of the PHITS code using the JENDL-HE file. To understand some discrepancies, more detailed analysis was needed.

Acknowledgment

The authors express their gratitude to staff of the Los Alamos Neutron Science Center at the Los Alamos National Laboratory. This facility is funded by the US Department of Energy.

References

- 1) K. Ishibashi, H. Takada, T. Nakamoto, *et al.*, "Measurement of neutron-production double-differential cross sections for nuclear spallation reaction induced by 0. 8, 1. 5 and 3. 0 GeV protons," *J. Nucl. Sci. Technol.* **34**[6], 529–537,(1997).
- 2) S. Leray, F. Borne, S. Crespin, *et al.*, "Spallation neutron production by 0.8, 1.2, and 1.6 GeV protons on various targets," *Phys. Rev.*, **C65**[4], 044621(2002).
- 3) W. B. Amian, R. C. Byrd, C. A. Goulding, *et al.*, "Differential Neutron Production Cross Sections for 800-MeV Protons," *Nucl. Sci. Eng.*, **112**, 78–86(1992).
- 4) S. A. Wender, S. Balestrini, A. Brown, *et al.*, "A fission ionization detector for neutron flux measurements at a spallation source," *Nucl. Instrum. Methods*, **A336**, 226–231(1993).
- 5) P. W. Lisowski, A. Gavron, W. E. Parker, *et al.*, "Fission cross sections in the intermediate energy region," *Proc. Specialists' Meeting on Neutron Cross Section Standards for the Energy Region above 20 MeV*, Uppsala, Sweden 21–23(1991).
- 6) G. Dietze, H. Klein, "Gamma-calibration of NE 213 scintillation counters," *Nucl. Instrum. Methods*, **193** 549–556(1982).
- 7) N. Nakao, T. Nakamura, M. Baba, *et al.*, "Measurements of response function of organic liquid scintillator for neutron energy range up to 135 MeV," *Nucl. Instrum. Methods*, **A362**, 454–465(1995).
- 8) D. Satoh, T. Sato, N. Shigyo, *et al.*, "SCINFUL-QMD: Monte Carlo based computer code to calculate response function and detection efficiency of a liquid organic scintillator for neutron energies up to 3 GeV," JAEA-Data/Code, 2006-023(2006).
- 9) H. Kitsuki, K. Ishibashi, N. Shigyo, *et al.*, "Parameterization of proton-induced neutron production double differential cross section up to 3 GeV in terms of moving source model," *J. Nucl. Sci. Technol.*, **38**[1], 1–7(2001).
- 10) T. Nakagawa, Y. Oyanagi, "Program system SALS for nonlinear least-squares fitting in experimental sciences," *Recent Developments in Statistical Inference and Data Analysis*. K. Matusita, editor. North Holland Publishing, Amsterdam, The Netherlands 221–225(1980).
- 11) H. Iwase, K. Niita, T. Nakamura, "Development of General-Purpose Particle and Heavy Ion Transport Monte Carlo Code," *J. Nucl. Sci. Technol.*, **39**[11] 1142–1151(2002).
- 12) T. Fukahori, Y. Watanabe, N. Yoshizawa, *et al.*, "JENDL High Energy File" *J. Nucl. Sci. Technol.*, **Suppl 2**, 25–30(2002).